


**Probing individual tunneling fluctuators with coherently controlled tunneling systems**Saskia M. Meißner,<sup>1</sup> Arnold Seiler,<sup>1</sup> Jürgen Lisenfeld,<sup>1</sup> Alexey V. Ustinov,<sup>1,2</sup> and Georg Weiss<sup>1</sup><sup>1</sup>*Physikalisches Institut, Karlsruher Institut für Technologie (KIT), D-76128 Karlsruhe, Germany*<sup>2</sup>*Russian Quantum Center, National University of Science and Technology MISIS, Moscow 119049, Russia* (Received 5 December 2017; revised manuscript received 22 December 2017; published 25 May 2018)

Josephson junctions made from aluminum and its oxide are the most commonly used functional elements for superconducting circuits and qubits. It is generally known that the disordered thin film  $\text{AlO}_x$  contains atomic tunneling systems. Coherent tunneling systems may couple strongly to a qubit via their electric dipole moment, giving rise to spectral level repulsion. In addition, slowly fluctuating tunneling systems are observable when they are located close to coherent ones and distort their potentials. This interaction causes telegraphic switching of the coherent tunneling systems' energy splitting. Here, we measure such switching induced by individual fluctuators on timescales from hours to minutes using a superconducting qubit as a detector. Moreover, we extend the range of measurable switching times to millisecond scales by employing a highly sensitive single-photon qubit SWAP spectroscopy and statistical analysis of the measured qubit states.

DOI: [10.1103/PhysRevB.97.180505](https://doi.org/10.1103/PhysRevB.97.180505)

Tunneling systems (TSs) are well known to govern the low-temperature properties of glasses, and a quite generally accepted description is provided by the standard tunneling model [1,2]. TSs are modeled as two-state systems created by atoms or small groups of atoms residing in double-well potentials. A sufficient overlap of the two localized wave functions results in two coherent states across the two wells. Their energy splitting is  $E = \sqrt{\varepsilon^2 + \Delta^2}$  with the asymmetry  $\varepsilon$  and the tunneling energy  $\Delta$ . Interaction with the environment is established via a variation of the asymmetry energy  $\varepsilon$  by strain and electric fields.

Coherent TSs can thus be resonantly driven by high-frequency strain or electric fields between their ground and excited states which correspond to symmetric and antisymmetric superpositions of the two localized wave functions, respectively. Incoherent TSs or two-level fluctuators (TLFs), according to the more general interpretation used in literature) may be defined as being essentially localized in either potential well with a rather low probability of tunneling to the other well [3]. The phase of the wave functions is destroyed between subsequent tunneling events [4,5]. The resulting random telegraphlike occupation of the two positions exerts strain or electric field fluctuations of the local environment which in turn may change the properties of other nearby TSs [6].

Here, we employ a phase qubit [7] consisting of a capacitively shunted Josephson junction embedded in a superconducting loop to resonantly measure the state of coherent TSs present in the disordered  $\text{AlO}_x$  barrier of the junction. These TSs act as detectors for nearby incoherent TLFs. Being subject to the fluctuating local fields, they exhibit jumps of their energy splitting through abrupt shifts of  $\varepsilon$ . The qubit energy is tuned by a flux bias and its state is controlled by externally applied microwave pulses at frequencies between 6 and 10 GHz. Details of the experimental setup are given by Lisenfeld *et al.* [8,9].

Additionally, the energy of both TSs and TLFs can be tuned by a static strain field which we create by bending the

chip with a piezostack [9]. Occasionally, the bending induces irreversible or hysteretic changes of the energy of individual TSs directly supporting the picture of locally confined TS-TLF interactions [6].

One method to observe slow TLFs with rather long dwell times (times  $\tau$  between two switching events) is to repeatedly measure the resonance curve of an affected TS [Fig. 1(a)] by exciting it with a long microwave pulse of frequency  $f_{\mu\text{w}}$  around its resonance (saturation spectroscopy). The excitation of the TS is transferred to the qubit during a SWAP pulse, followed by a qubit state readout [see Fig. 1(b)]. Figure 1(a) shows the resulting probability  $P(|1\rangle)$  of the qubit being excited by the TS, which in turn was saturated with the long microwave pulse, together with Lorentzian fits, for two frequency sweeps taken a few minutes apart. The TS center frequency  $f_{\text{TS}}$  was extracted from each resonance and plotted as a function of time in Fig. 1(c), clearly showing telegraphic switching between two frequency values. This is interpreted as abrupt changes of the TS's asymmetry energy caused by the fluctuating local strain or electric fields belonging to the two microscopic configurations of a nearby TLF. Due to the incoherent nature of the TLF, the local fields which it exerts on the TSs are treated classically as being quasistatic [6]. A measure of the coupling strength between TS and TLF is given by the difference between the two resonance frequencies, which in this case is of about 14 MHz. (This may not be confused with the coupling of two coherent TSs.) The histograms of the population probabilities of the TLF  $|L\rangle$  and  $|R\rangle$  states [Fig. 1(d)] allows one to extract more information about the causative TLF that is not directly visible to the qubit. Using Boltzmann statistics on the ratio of the dwell times in the localized states of the TLF, one can calculate the energy splitting  $E_{\text{TLF}} \approx h \times 0.6 \text{ GHz} = k_{\text{B}} \times 30 \text{ mK}$  by

$$\frac{\langle \tau_{|R\rangle} \rangle}{\langle \tau_{|L\rangle} \rangle} = \exp\left(-\frac{E_{\text{TLF}}}{k_{\text{B}} T}\right). \quad (1)$$

Changing the static strain by slightly increasing the voltage of the piezostack results in  $E_{\text{TLF}} = k_{\text{B}} \times 50 \text{ mK}$  which indicates

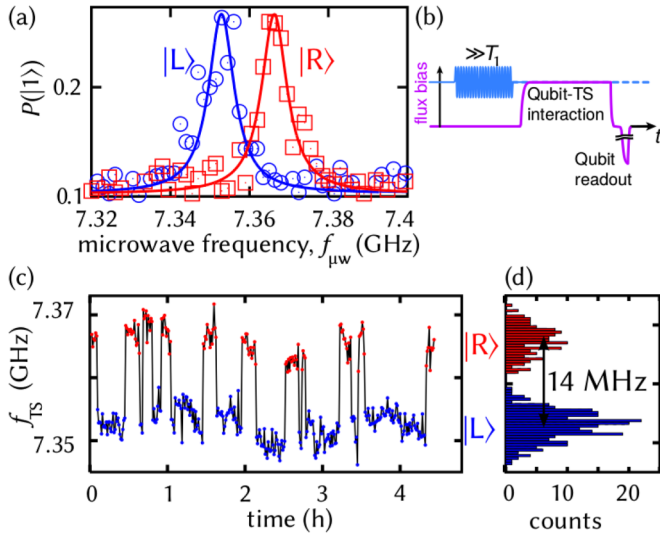


FIG. 1. Energy fluctuation of a TS resonance  $f_{TS}$  due to a TLF. (a) The TS resonances are measured by application of a long microwave pulse  $f_{\mu w}$  observing the qubit population  $P(|1\rangle)$  after aSWAP pulse as shown in the pulse sequence (b). Each data point comprises 1000 single measurements within 0.7 s. (c) Random telegraphic noise of the TS resonance measured at 40 mK. (d) Histograms of the population probabilities of the TLF's  $|L\rangle$  and  $|R\rangle$  states.

that  $E_{TLF}$  depends on the asymmetry and is tunable by strain similar to coherent TSs [9]. The TLF's slow fluctuation rate points towards a small tunneling energy  $\Delta_{TLF} \ll k_B T$ . Therefore, the energy splitting is given mainly by the asymmetry energy, where  $E_{TLF} \approx \epsilon_{TLF} \approx k_B T$  is comparable to the temperature  $T = 40$  mK of the sample.

The additional small drift of the resonance frequency of the TS in Fig. 1(c) can be attributed to a larger bath of very weakly coupled TLFs and may be discussed in terms of spectral diffusion [10]. This effect has recently been attributed to causing frequency fluctuations of superconducting resonators [11–14], time-dependent fluctuations of qubit energy relaxation rates [15], and dephasing of high-frequency TSs [16,17].

If a TLF switches between its states faster than the time  $\tau_M = 0.7$  s required to measure the averaged qubit state probability, both resonance frequencies of the coherent TS appear simultaneously. Such a situation is depicted in Fig. 2(a) with a larger overview in Ref. [6]. These data were acquired using single-photon SWAP spectroscopy [18] by applying the pulse sequence shown in Fig. 2(b). Dark traces correspond to a reduced probability to measure the excited state of the qubit, which indicates that the excitation of the qubit was transferred to a TS.

The resulting change of the TS's hyperbolic trace corresponds to a shift along the strain axis, indicating that the coupling to the TLF only affects the TS's asymmetry and not its tunneling energy. For the two parallel TS resonances  $E_1$  and  $E_2$  (gray and black hyperbolas), which are simultaneously visible only in a small range of mechanical deformation [Fig. 2(a)], the suggested potential of the TLF (magenta hyperbola) strongly depends on external strain. Coming from a highly asymmetric potential configuration where it is trapped most of the time in one configuration, the TLF passes through its symmetry point

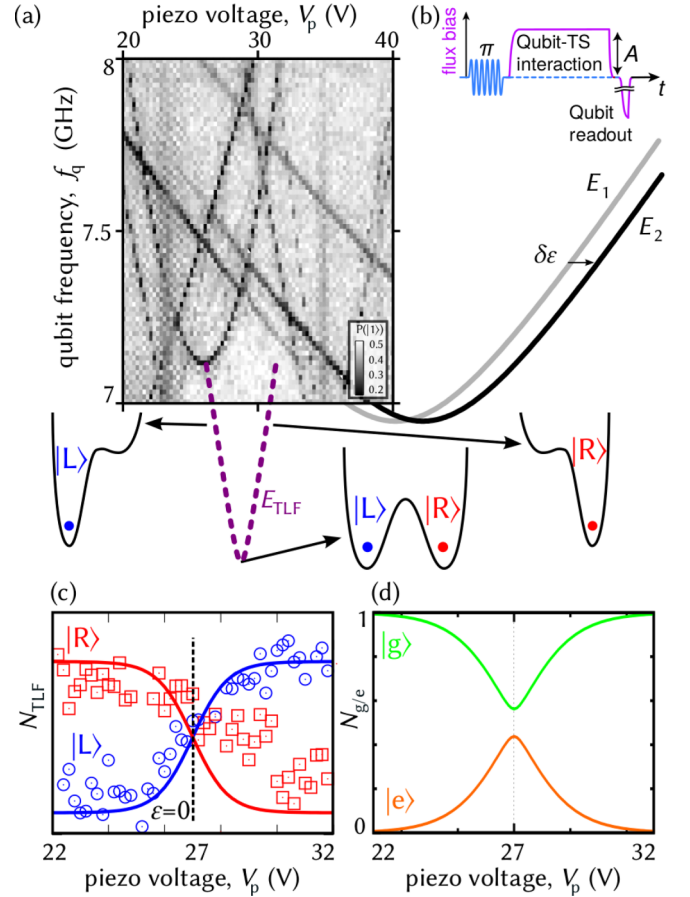


FIG. 2. Strain dependence of TS resonance frequencies: (a) Dark traces correspond to a reduced qubit population indicating that the qubit lost its excitation to a coherent TS. Particular attention is owed to the two parallel TS traces in the middle of the plot with a smooth transition from  $E_1$  to  $E_2$  continued as gray and black hyperbolas. The sketches show the suggested TLF energy  $E_{TLF}$  (magenta, energy not to scale) and three variations of its double-well potential. (b) Protocol for single-photon SWAP spectroscopy. The qubit is excited by a  $\pi$  pulse and subsequently tuned to a range of frequencies  $f_q$  to find TSs. (c) Occupation number  $N_{TLF}$  and (d) in energy basis  $N_{g/e}$  as a function of strain at 40 mK with continuous lines obeying Eqs. (2) and (3).

and finally ends up in the other configuration, for convenience labeled  $|L\rangle$  and  $|R\rangle$ , respectively. Both traces of the resonant TS visible to the qubit are described by the same hyperbola only shifted by a mechanical distortion corresponding to a change of the piezovoltage of 2.45 V. The changes in the grayscale density of the two TS traces correspond to the change in the  $|L\rangle|R\rangle$  occupancy of the TLF.

From the qubit population extracted along the two branches in Fig. 2(a) we obtain the occupancy probability  $N_{TLF}$  of the TLF being in either configuration as a function of mechanical deformation [Fig. 2(c)]. This is described by the projection of the density matrix onto the localized basis,

$$N_{TLF_{L/R}} = \frac{\Delta^2}{2(E^2 \pm \epsilon E)} \left[ N_g + \left( \frac{E \pm \epsilon}{\Delta} \right)^2 N_e \right], \quad (2)$$

where

$$N_{g/e} = \frac{1}{2} \left[ 1 \pm \tanh \left( \frac{E}{2k_B T} \right) \right] \quad (3)$$

is the occupation number in the energy basis [Fig. 2(d)].

Although we cannot resolve telegraph switching for this rather fast TLF, there is a way to extract information about its switching rate using a statistical analysis of many subsequent individual qubit measurements. In principle, the data can be analyzed as well in the framework of autocorrelation [19]. Here, we prefer to simulate the statistics as a direct comparison to the measurement.

In the following, we present such a statistical analysis and a corresponding simulation using a sequence of  $N_0 = 50\,000$  successive single measurements. Figure 3(a) shows a series of successive individual measurements of the readout dc superconducting quantum interference device's (SQUID's) switching current which depends on the excitation probability of the qubit. By defining a threshold value of  $64.4 \mu\text{A}$  indicated by a red line, we attribute each switching current with a contrast of about 95% as described in Ref. [20] to one of the two qubit states as shown by the gray digital data and right vertical axis. Figure 3(b) shows the qubit excitation probability, where the qubit was biased to different resonance frequencies  $f_q$  averaged from 50 000 measurements for each  $f_q$ . Due to energy relaxation which occurs at a rate of  $T_1^{-1} \approx 1/100$  ns during the 40-ns-long qubit-TS interaction time [see Fig. 2(b)], the qubit remains at a maximum excitation probability of  $P(|1\rangle) \approx 0.5$  when it is not in resonance with a strongly coupled TS. In contrast, at a frequency of  $f_q = 6.72$  GHz, a resonant interaction with a TS results in a reduced excitation probability of  $P^*(|1\rangle) = 0.32$  since the energy was transmitted to the TS with a certain probability.

The probabilities  $P(|1\rangle)$  and  $P(|0\rangle)$  to measure the excited or the ground state of the qubit, respectively, are given by a Bernoulli distribution [21] with two possible outcomes and  $P(|0\rangle) + P(|1\rangle) = 1$ . One finds that the numerical simulation of our coupled detector system is similar to the statistics problem of tossing a biased coin for which  $P(|0\rangle) \neq P(|1\rangle)$ . In the case of independent individual measurements, a closed expression for the abundance  $N(m)$  of exactly  $m$  successive measurements which have the same result is described by a Bernoulli distribution for  $m \ll N_0$ ,

$$\ln [N(m)] = m \ln(p) + \ln(N_0) + 2 \ln(1 - p), \quad (4)$$

where  $p$  is either  $P(|1\rangle)$  or  $P(|0\rangle)$  (see Supplemental Material [6]). Therefore, the abundance  $N(m)$  of measuring  $m$  times the same qubit state results in two histograms for the qubit's ground  $|0\rangle$  (green) and excited  $|1\rangle$  (orange) state which are depicted in Fig. 3(c) for the isolated qubit and Fig. 3(d) for the qubit interacting with one coherent TS. Thus, the slope of the straight black lines using Eq. (4) in a logarithmic plot coincides with the measured probabilities (Fig. 3) for both analyzed frequencies  $f_q$ .

This indicates that the statistics for the case of an isolated qubit and for the case of the qubit in resonance with a TS are both described by a Bernoulli process, proving the independence of subsequent events, where, however, the latter case results in an increased decay probability of the qubit.

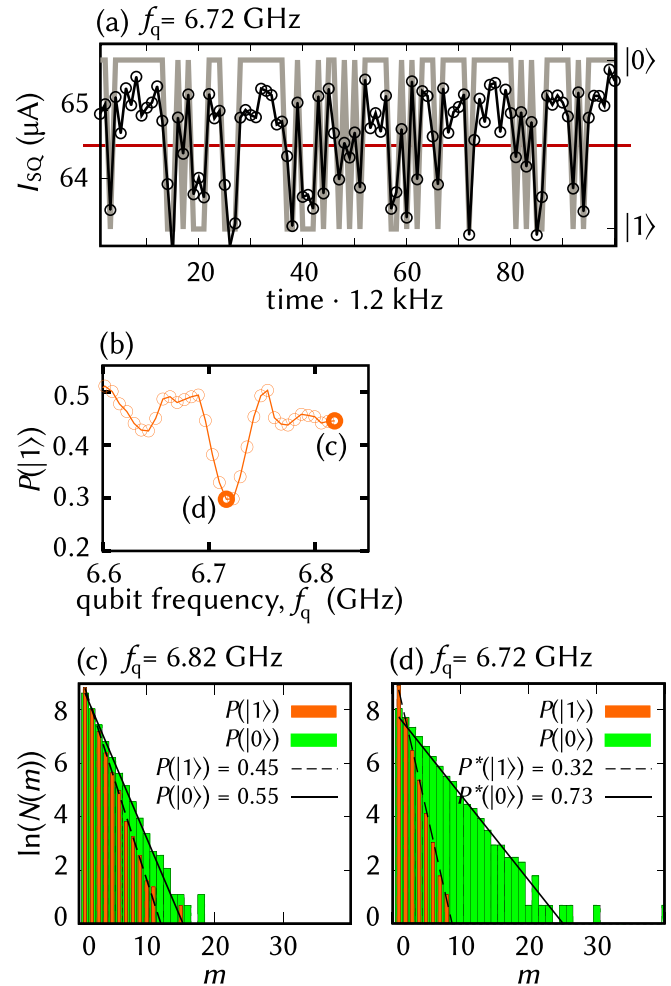


FIG. 3. (a) 100 out of 50 000 single measurements of the readout dc-SQUID's switching current  $I_{SQ}$  (black line, left axis) and the associated qubit states  $|0\rangle$  and  $|1\rangle$  (gray line, right axis). (b) Qubit population probability  $P(|1\rangle)$  for resonant excitation when it was tuned to different resonance frequencies  $f_q$ . The dip at  $f_q = 6.72$  GHz indicates a resonant interaction with a coherent TS. (c) and (d) show the abundances  $\ln[N(m)]$  of measuring  $m$  successive times the same qubit state  $P(|0\rangle)$  (green) or  $P(|1\rangle)$  (orange), taken either for the isolated qubit (c) or the qubit in resonance with the TS (d). For the latter case, the qubit is found with a larger probability of  $P^*|0\rangle$  in its ground state. Continuous and dashed lines are fits to Eq. (4). Deviations from the unity of the sum of probabilities are due to statistical uncertainty using a finite number of measurements.

Now the statistical analysis is applied to a coupled system consisting of the qubit and a coherent TS which is additionally modulated by a TLF. In Fig. 4(a) another example of two TS resonance traces as a function of mechanical deformation is shown. A vertical cut of this plot close to the symmetry point of the TLF is depicted in Fig. 4(b) where the two highlighted data points are analyzed further. As shown in Fig. 4(c), the abundance  $N(m)$  of measuring  $m$  times the same qubit state results in two histograms for the qubit's ground  $|0\rangle$  (orange) and excited  $|1\rangle$  (green) states. The exponential abundance measured at  $f_q = 8$  GHz [Fig. 4(c)]  $N(m)$  agrees with Eq. (4), in accordance with the numerical simulation of an undisturbed Bernoulli process.

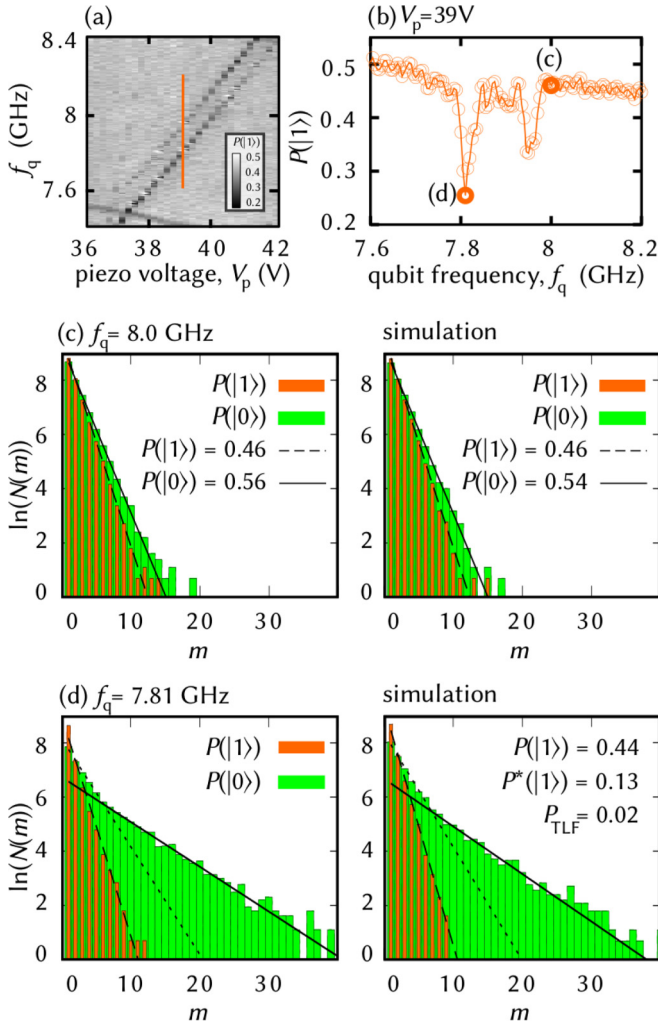


FIG. 4. (a) Two parallel TS traces as a function of mechanical deformation. (b) Line cut along the frequency axis (orange line) of (a) near the symmetry point of the TLF with two highlighted data points marked with (c) and (d) according to the following plots. (c) Statistic analysis using 50 000 single-qubit measurements and simulation of the qubit without perturbation: The abundance  $N(m)$  of measuring  $m$  times the same qubit state results in two histograms for the qubit's ground  $|0\rangle$  (green) and excited  $|1\rangle$  state (orange), and black dashed lines are fits with Eq. (4). (d) Analysis of a coherent TS which is disturbed by an incoherent TLF: The switching probability  $P_{\text{TLF}}$  is determined by comparison of the simulation with the experimental data (black lines are only guides to the eye).

Analysis of a TS which is coupled to an incoherent TLF reveals a correlation of subsequent single measurements of the qubit state. The correlation manifests itself as a kink in the histogram of Fig. 4(d) measured at  $f_q = 7.81$  GHz, where the qubit is in resonance with the TS. The coupled system of the qubit, the TS, and the TLF is simulated by a coin toss with two differently biased coins. One coin with a specific probability  $P^*$  describes the qubit and the TS. Another coin with  $P$  describes the qubit without perturbation, where the TLF has shifted the TS out of resonance with the qubit. With a certain probability  $P_{\text{TLF}}$ , the TLF exchanges the two coins between two single measurements in the series of

$N_0$  measurements, so that either  $P$  or  $P^*$  is measured (see Supplemental Material [6]). This simulation is used in Fig. 4(d) where the switching probability  $P_{\text{TLF}}$  of the TLF is determined by adjusting the simulation parameters until agreement with the experimental data is found. We want to note that the TLF switching rates from  $|R\rangle$  to  $|L\rangle$  and vice versa in general are not equal but depend on their energetic difference. However, since the observed TLF is close to its symmetry point ( $\varepsilon_{\text{TLF}} \approx 0$ ), we can treat them as being approximately equal.

The extracted probability  $P_{\text{TLF}} = (0.02 \pm 0.01)$  and the repetition rate of 1.2 kHz results with  $\tau_{\text{TLF}}^{-1} = 1.2 \text{ kHz} \times P_{\text{TLF}}$  in a fluctuation rate of

$$\tau_{\text{TLF}}^{-1} = 1/(38 \pm 17) \text{ ms}. \quad (5)$$

When comparing the experiment with the coin toss simulation, the observation of the characteristic kink is crucial, and the position of the kink mainly depends on  $P_{\text{TLF}}$  [6]. Clearly, the determination of decay rates with such a (statistical) method has an upper bound given by the repetition rate of the experiment. Here, the repetition rate is limited by the initialization and readout of the qubit. Faster methods might be possible with dispersive readout protocols [22] that allow repetition rates of  $\approx 1\text{--}10$  MHz.

In conclusion, individual TLFs in the  $\text{AlO}_x$  of Josephson junction tunnel barriers and their switching dynamics are measured through a two-stage detection involving their coupling to a coherent TS which itself is coupled to a qubit. Various existing methods to characterize slow TLFs, e.g., conductance fluctuations, are limited to fluctuation rates  $\lesssim 1 \text{ s}^{-1}$  due to the averaging time of the measuring system [23–25]. Here, we have described a method to measure much faster fluctuation rates which we estimate to reach 1/8 ms [6]. This value is in agreement with a rough estimate of the fastest fluctuation rates of TLFs at a given temperature [26]. The investigated fluctuator also confirms the finding that one individual TLF is sufficient to severely limit the coherence of a nearby TS [17]. We like to point out that apparently the same fundamental mechanism, namely, strain field or electric field mediated direct interaction between atomic tunneling systems, may be responsible for an extremely broad spectrum of noise affecting the coherence of virtually any quantum system or circuitry. The experiments discussed in this Rapid Communication demonstrate fluctuation rates in the kHz range bridging the huge gap between conductance fluctuations in the Hz range and the MHz range explored by echo experiments. The existence of this broad noise spectrum is not only relevant for dephasing of quantum systems, but also in the more general aspect of atomic tunneling systems in disordered matter and their dynamics induced by interactions.

We would like to thank J. M. Martinis (UCSB) for providing us with the sample that we measured in this work, as well as D. Hunger and S. Matityahu for fruitful discussions. Support by the Deutsche Forschungsgemeinschaft (DFG) (Grant No. LI 2446/1-1) is gratefully acknowledged, as well as partial support by the Ministry of Education and Science of Russian Federation in the framework of Increase Competitiveness Program of the National University of Science and Technology (NUST) MISIS (Contract No. K2-2017-081).

- [1] W. A. Phillips, *J. Low Temp. Phys.* **7**, 351 (1972).
- [2] P. W. Anderson, B. I. Halperin, and C. M. Varma, *Philos. Mag.* **25**, 1 (1972).
- [3] C. Müller, J. H. Cole, and J. Lisenfeld, [arXiv:1705.01108](https://arxiv.org/abs/1705.01108).
- [4] A. Würger, R. Weis, M. Gaukler, and C. Enss, *Europhys. Lett.* **33**, 533 (1996).
- [5] R. Egger, H. Grabert, and U. Weiss, *Phys. Rev. E* **55**, R3809 (1997).
- [6] See Supplemental Material at <http://link.aps.org/supplemental/10.1103/PhysRevB.97.180505> for the interaction of TSs with TLFs, local hysteresis of TSs due to TLFs, fast TLFs, and a statistical analysis.
- [7] M. Steffen, M. Ansmann, R. McDermott, N. Katz, R. C. Bialczak, E. Lucero, M. Neeley, E. M. Weig, A. N. Cleland, and J. M. Martinis, *Phys. Rev. Lett.* **97**, 050502 (2006).
- [8] J. Lisenfeld, C. Müller, J. H. Cole, P. Bushev, A. Lukashenko, A. Shnirman, and A. V. Ustinov, *Phys. Rev. Lett.* **105**, 230504 (2010).
- [9] G. J. Grabovskij, T. Peichl, J. Lisenfeld, G. Weiss, and A. V. Ustinov, *Science* **338**, 232 (2012).
- [10] J. L. Black and B. I. Halperin, *Phys. Rev. B* **16**, 2879 (1977).
- [11] L. Faoro and L. B. Ioffe, *Phys. Rev. B* **91**, 014201 (2015).
- [12] J. Burnett, L. Faoro, I. Wisby, V. L. Gurtovoi, A. V. Chernykh, G. M. Mikhailov, V. A. Tulin, R. Shaikhaidarov, V. Antonov, P. J. Meeson, A. Y. Tzalenchuk, and T. Lindström, *Nat. Commun.* **5**, 4119 (2014).
- [13] A. L. Burin, S. Matityahu, and M. Schechter, *Phys. Rev. B* **92**, 174201 (2015).
- [14] M. S. Khalil, F. C. Wellstood, and K. D. Osborn, *IEEE Trans. Appl. Supercond.* **21**, 879 (2011).
- [15] C. Müller, J. Lisenfeld, A. Shnirman, and S. Poletto, *Phys. Rev. B* **92**, 035442 (2015).
- [16] S. Matityahu, A. Shnirman, G. Schön, and M. Schechter, *Phys. Rev. B* **93**, 134208 (2016).
- [17] J. Lisenfeld *et al.*, *Sci. Rep.* **6**, 23786 (2016).
- [18] J. Lisenfeld, G. Grabovskij, C. Müller, J. H. Cole, G. Weiss, and A. V. Ustinov, *Nat. Commun.* **6**, 6182 (2015).
- [19] E. L. Elson, *Biophys. J.* **101**, 2855 (2011).
- [20] J. Lisenfeld, A. Lukashenko, and A. V. Ustinov, *Appl. Phys. Lett.* **91**, 232502 (2007).
- [21] V. Uspensky, *Introduction to Mathematical Probability* (McGraw-Hill, New York, 1937).
- [22] T. Walter *et al.*, *Phys. Rev. Appl.* **7**, 054020 (2017).
- [23] K. Chun and N. O. Birge, *Phys. Rev. B* **48**, 11500 (1993).
- [24] S. Brouër, G. Weiss, and H. B. Weber, *Europhys. Lett.* **54**, 654 (2001).
- [25] S.-S. Yeh, W.-Y. Chang, and J.-J. Lin, *Sci. Adv.* **3**, e1700135 (2017).
- [26] J. Jäckle, *Z. Phys.* **257**, 212 (1972).